University of South Carolina
Department of Chemistry

CHEM 749 Spring 2020:
Chemistry and Physics of Low-Dimensional Materials
Andrew Greytak

Supplement to Lecture 6: Graphene and Carbon Nanotube Band Structure from Tight Binding

---

Tight-binding result

The tight-binding calculation of the graphene band structure (see Wallace 1947 [1], Saito et al. 1992 [2], Castro Neto et al. 2009 [3]) is more complicated than that for our 1-D s-orbital chain both because it's in two dimensions, and because there are two atoms per unit cell (two atoms per Bravais lattice site). This two-atom *basis* means there are effectively two hexagonal lattices formed by two sets of atoms A and B. Bloch wavefunctions ψ_A and ψ_B describe states formed from the p_z orbitals on atoms in lattices A and B (ϕ_A and ϕ_B), but the actual band states are linear combinations of these:

$$\psi_{A,k} = \sum_A e^{i\mathbf{k}\cdot\mathbf{R}_A}\phi_A(\mathbf{r}-\mathbf{R}_A) \tag{1}$$

$$\psi_{B,k} = \sum_B e^{i\mathbf{k}\cdot\mathbf{R}_B}\phi_B(\mathbf{r}-\mathbf{R}_B) \tag{2}$$

$$\Psi_k = c_{A,k}\psi_{A,k} + c_{B,k}\psi_{B,k} \tag{3}$$

and we want to find coefficients $c_{i,k}$ such that

$$\mathbf{H}\Psi_k = E_k\Psi_k \tag{4}$$

To find the band energies E_k according to the variational principle, we must solve the following "secular determinant":

$$\begin{vmatrix} H_{AA}-E\,S_{AA} & H_{AB}-E\,S_{AB} \\ H_{BA}-E\,S_{BA} & H_{BB}-E\,S_{BB} \end{vmatrix} = 0 \tag{5}$$

Where H_{ij} and S_{ij} represent the interaction and overlap integrals between each basis Bloch function. We require that $H_{AB} = H_{BA}^*$ and $S_{AB} = S_{BA}^*$. The problem is greatly simplified for graphene by noting that all of the atomic orbitals are the same so $H_{AA} = H_{BB} = H_{11}$. We can further simplify by neglecting overlap ($S_{AA} = S_{BB} = 1$ and $S_{AB} = 0$). As described by Wallace, the nearest-neighbor correction to the atomic orbital energies then becomes:

$$E_{2\mathrm{D}} = H_{11} \pm H_{12} \tag{6}$$

$$H_{11} = E_\circ - \gamma_\circ' \sum_{A,A=\mathrm{n.n.}} e^{i\mathbf{k}(\mathbf{R}_{A'}-\mathbf{R}_A)} \tag{7}$$

$$H_{BA} = -\gamma_\circ \sum_{A,B=\mathrm{n.n.}} e^{i\mathbf{k}(\mathbf{R}_B-\mathbf{R}_A)} \tag{8}$$

$$H_{12} = [H_{BA}H_{BA}^*]^{1/2} \tag{9}$$

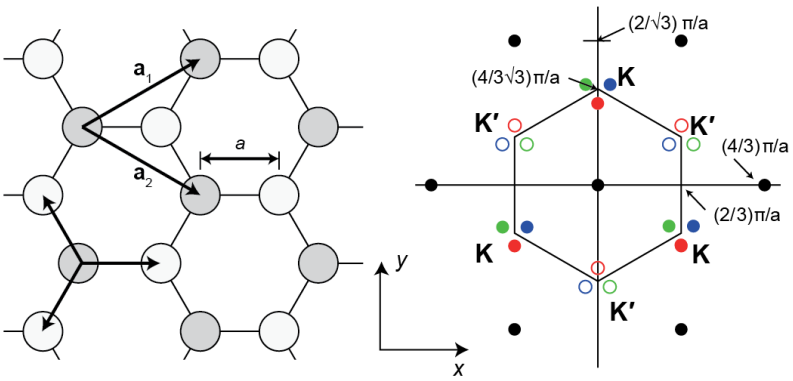

Figure 1: *Left:* The graphene lattice. The two groups of like atoms are differently shaded. Representative primitive lattice vectors and nearest-neighbor vectors are shown. *Right:* Reciprocal space. The black dots describe reciprocal lattice points. The black line marks the extent of the first Brillouin zone. The colored circles near the $\mathbf{K}$ and $\mathbf{K}'$ points help to identify regions that describe the same states: Each filled red circle describes the same state. The filled and open circles of each color describe two sets of states that are linked by inversion symmetry. It can be seen that the Brillouin zone includes exactly one instance of each of these points, completely describing the region surrounding each of the two distinct $\mathbf{K}$ points.

where H_{11} accounts for nearest neighbors within the same Bravais lattice (i.e. two bonds away, and includes an on-site term) and H_{12} accounts for nearest neighbors in different Bravais lattices (i.e. one bond away). In the crudest treatment, H_{11} can be neglected. The $+$ and $-$ in Equation 6 refer to the valence and conduction bands respectively, and $-\gamma_\circ$ and $-\gamma'_\circ$ are the nearest-neighbor interaction integrals (written such that $\gamma_\circ$ and $\gamma'_\circ$ have positive values, which follows the convention used by Wallace and Geim). Inspection of the graphene lattice shows that for a given atom, there are six nearest-neighbor Bravais lattice vectors $\mathbf{R}_{AA'}$. In what follows, a is the **bond length**, so that $a\sqrt{3}$ is length of a primary lattice vector (the lattice constant). This is the convention of Geim *et al.* The $\mathbf{R}_{AA'}$ are:

$$\mathbf{R}_{A'} - \mathbf{R}_A = \pm\sqrt{3}a\hat{\mathbf{y}} \tag{10}$$

$$\mathbf{R}_{A'} - \mathbf{R}_A = \pm\frac{3}{2}a\hat{\mathbf{x}} \mp \frac{\sqrt{3}}{2}a\hat{\mathbf{y}} \tag{11}$$

$$\mathbf{R}_{A'} - \mathbf{R}_A = \pm\frac{3}{2}a\hat{\mathbf{x}} \mp \frac{\sqrt{3}}{2}a\hat{\mathbf{y}} \tag{12}$$

$$\tag{13}$$

while there are three nearest-neighbor vectors $\mathbf{R}_{AB}$ between atoms on the two different sites:

$$\mathbf{R}_B - \mathbf{R}_A = a\hat{\mathbf{x}} \tag{14}$$

$$\mathbf{R}_B - \mathbf{R}_A = -\frac{a}{2}\hat{\mathbf{x}} + \frac{\sqrt{3}}{2}a\hat{\mathbf{y}} \tag{15}$$

$$\mathbf{R}_B - \mathbf{R}_A = -\frac{a}{2}\hat{\mathbf{x}} - \frac{\sqrt{3}}{2}a\hat{\mathbf{y}} \tag{16}$$

$$\tag{17}$$

Then,

$$H_{11} = E_\circ - \gamma'_\circ\left[2\cos(k_y\sqrt{3}a) + 4\cos(k_x\frac{3}{2}a)\cos(k_y\frac{\sqrt{3}}{2}a)\right] \tag{18}$$

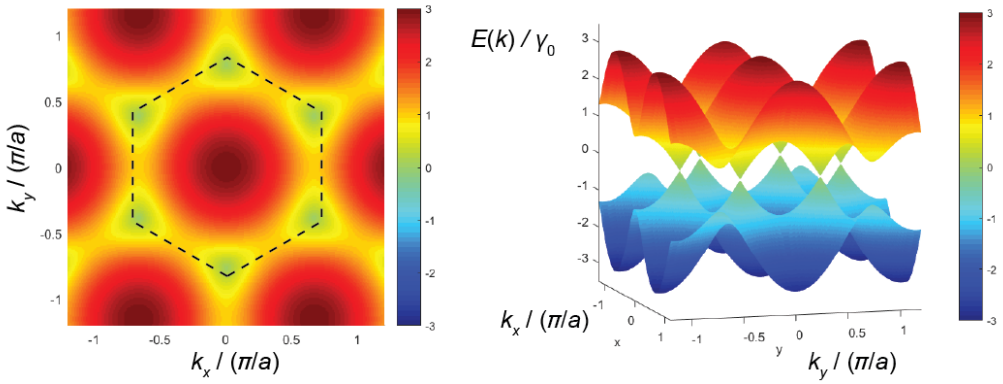

Figure 2: *Left:* Top view of the conduction band of graphene, plotted with a color scale of energy. The Brillouin zone edge is highlighted. *Right:* A 3-D view of energy vs. k_x and k_y illustrating the two bands and the conical nature of the contact between bands at points $\mathbf{K}$ and $\mathbf{K}'$.

$$H_{BA} = \gamma_\circ \left[e^{ik_x a} + 2e^{-ik_x a/2} \cos(k_y \frac{\sqrt{3}}{2} a) \right] \tag{19}$$

$$H_{12} = [H_{BA}^* H_{BA}]^{1/2} = \gamma_\circ \left[1 + 4\cos(k_x \frac{3}{2} a) \cos(k_y \frac{\sqrt{3}}{2} a) + 4\cos^2(k_y \frac{\sqrt{3}}{2} a) \right]^{1/2} \tag{20}$$

It's possible to write these more concisely as

$$H_{11} = E_\circ - \gamma'_\circ f(\mathbf{k}) \tag{21}$$

$$H_{12} = -\gamma_\circ \sqrt{3 + f(\mathbf{k})} \tag{22}$$

with

$$f(\mathbf{k}) = 2\cos(k_y \sqrt{3} a) + 4\cos(k_x \frac{3}{2} a) \cos(k_y \frac{\sqrt{3}}{2} a) \tag{23}$$

Importantly, this works out to $E_{2D} = E_\circ \pm 3\gamma_\circ - 6\gamma'_\circ$ at $\mathbf{k} = 0$, where the $+$ version represents the upper (conduction) band and the $-$ version the lower (valence band). The bands are degenerate for $\mathbf{k}$'s at the six corners of the Brilloiun zone with $E_{2D} = E_\circ + 3\gamma'_\circ$ (for example, try $\mathbf{k} = \frac{4}{3\sqrt{3}} \frac{\pi}{a} \hat{\mathbf{y}}$). The Brillouin zone contacts six such points, which are typically labeled K. We expect $\gamma_\circ > \gamma'_\circ$ because the AB distances are shorter, and in fact the essential behavior can be understood by considering $\gamma'_\circ = 0$ (ignoring H_{11}).

We can plot this band structure as a three-dimensional surface, with energy on the vertical scale. The fact that the points of contact between the valence and conduction band fall at the edge of the Brillouin zone make it tricky to visualize, and count, the regions of $\mathbf{k}$ space that are close to the band edge in this system. It will be easiest to see the form of the conical band structure around the K points if we use the "extended zone" scheme (continuing the band structure outside of the zone). This is perfectly fine as long as we remember that $\mathbf{k}$ values separated by a reciprocal lattice vector actually describe the same states. Thus there are evidently a total of *two* distinct points of contact between the bands; these points are labeled these $\mathbf{K}$ and $\mathbf{K}'$ in Figure 1. These are equivalent to each other by inversion symmetry, but the regions around each describe different states.

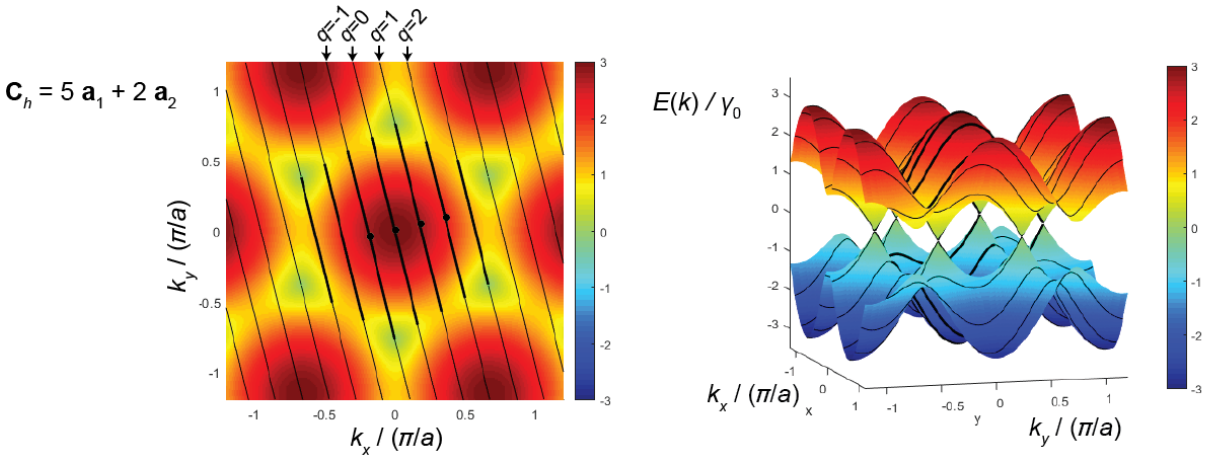

Figure 3: Allowed $\mathbf{k}$ vectors for a (5,2) nanotube. Each line corresponds to states with constant q and various values of t; t thus describes the wavevector along the nanotube axis. The black dots in the view at left indicate $\mathbf{k}$ for $t = 0$ for several representative subbands. As seen at right, each line of allowed $\mathbf{k}$ values describes a valence and conduction sub-bands. The thicker segments of the lines indicate portions of each subband that fall within the Brillouin zone and thus describe unique states. Because the $\mathbf{K}$ and $\mathbf{K}'$ points are included among the allowed $\mathbf{k}$ values, this nanotube is expected to be a metal.

Quantum confinement in single-walled carbon nanotubes

Now, we can go about imposing quantum confinement by declaring a roll-up vector $\mathbf{C}_h = n\mathbf{a}_1 + m\mathbf{a}_2$ with $\mathbf{a}_1$ and $\mathbf{a}_2$ primitive (direct) lattice vectors. The length of $\mathbf{C}_h$ is the circumference of the tube; a trip around the circumference must comprise an integer number of electron wavelengths, or in other words

$$\mathbf{C}_h \cdot \mathbf{k} = 2\pi q \tag{24}$$

where q is an integer. In other words, the component of $\mathbf{k}$ in the $\mathbf{C}_h$ direction must be an integer multiple of $2\pi/|\mathbf{C}_h|$. The component of $\mathbf{k}$ perpendicular to $\mathbf{C}_h$ could have any value: we will call it t.

$$\mathbf{k} = \frac{2\pi q}{|\mathbf{C}_h|}\hat{\mathbf{C}}_h + t(\perp \hat{\mathbf{C}}_h) \tag{25}$$

$$\hat{\mathbf{C}}_h = \frac{C_{h,x}}{|\mathbf{C}_h|}\hat{\mathbf{x}} + \frac{C_{h,y}}{|\mathbf{C}_h|}\hat{\mathbf{y}} \tag{26}$$

$$\perp \hat{\mathbf{C}}_h = -\frac{C_{h,y}}{|\mathbf{C}_h|}\hat{\mathbf{x}} + \frac{C_{h,x}}{|\mathbf{C}_h|}\hat{\mathbf{y}} \tag{27}$$

$$\tag{28}$$

where we have arbitrarily set $\perp \hat{\mathbf{C}}_h$ to be rotated to the 90° to the left vs. $\hat{\mathbf{C}}_h$. Now, we have a complete description of $\mathbf{k}$:

$$\mathbf{k} = \left(\frac{2\pi q C_{h,x}}{|\mathbf{C}_h|^2} - t\frac{C_{h,y}}{|\mathbf{C}_h|}\right)\hat{\mathbf{x}} + \left(\frac{2\pi q C_{h,y}}{|\mathbf{C}_h|^2} + t\frac{C_{h,x}}{|\mathbf{C}_h|}\right)\hat{\mathbf{y}} \tag{29}$$

Using Equation 29 we step through integer values of q, and for each one, we generate a line of $\mathbf{k}$'s by varying t continuously. At each $\mathbf{k}$, Equation 20 can be used to compute the valence and conduction band energy. This is exactly what is done to generate Figure 3, using $\mathbf{a}_1 = (3a/2)\hat{\mathbf{x}} + (a\sqrt{3}/2)\hat{\mathbf{y}}$ and $\mathbf{a}_2 = (3a/2)\hat{\mathbf{x}} - (a\sqrt{3}/2)\hat{\mathbf{y}}$ as the primitive lattice vectors.

The values of t and q can be positive, negative, or zero. For the figure, we set the limits of q and t to completely cover the limits of our plot. Of course, only values of $\mathbf{k}$ that actually fall within the Brillouin zone will describe unique states. If desired, this condition can be met by checking that:

$$|k_x| \leq \frac{2}{3}\frac{\pi}{a} \tag{30}$$

$$\frac{1}{\sqrt{3}}|k_x| + |k_y| \leq \frac{4}{3\sqrt{3}}\frac{\pi}{a} \tag{31}$$

The (n,m) = (5,2) nanotube described in Figure 3 is metallic. Figure 4 describes a (5,3) nanotube, which is a semiconductor since the valence and conduction subbands never touch.

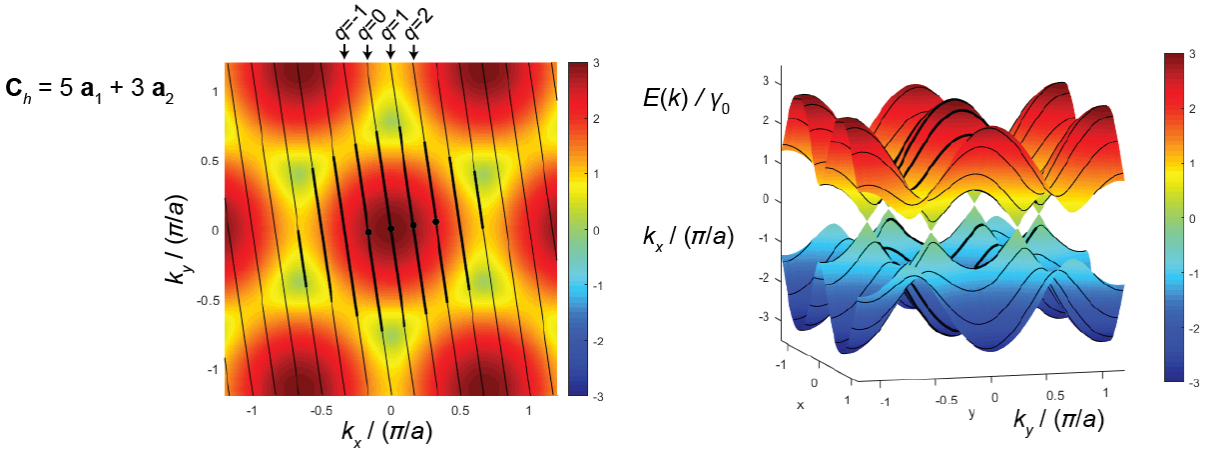

Figure 4: Allowed $\mathbf{k}$ vectors for a (5,3) nanotube. Because the $\mathbf{K}$ and $\mathbf{K}'$ points are not included among the allowed $\mathbf{k}$'s, this nanotube is expected to be a semiconductor. Note that the band-edge states are still close to the $\mathbf{K}$ and $\mathbf{K}'$ points, and that the nanotube is a direct bandgap semiconductor since the conduction subband minimum and valence subband maximum occur at the same value of $\mathbf{k}$.

There are several ways to plot the dispersion of the subbands along the nanotube axis. In Figure 5, the energy of the various subbands versus axial wavevector t is shown for the (5,2) and (5,3) examples. Looking carefully at the metallic (5,2) case, there are *two* unique subbands that are partially filled at the Fermi energy (remember $E_{\mathrm{F}} = 0$ here) ... for some value of E close to zero, each of these subbands intersects E twice (once for $t > 0$ and once for $t < 0$, corresponding to states propagating forwards and backwards along the tube axis) leading to a total of four states with $E = E_{\mathrm{F}}$. A similar situation is found in the semiconducting tube: there are two distinct conduction band minima and two distinct valence band maxima within the Brillouin zone, so if E_{F} is brought close to E_{C} or E_{V}, there will always be two subbands that are equally populated with carriers. Thus, in the strictest sense, carbon nanotubes are not one-dimensional electronic systems since there are always at least two 1-D subbands that participate! Nonetheless, the reduced dimensionality versus bulk graphite is keenly evidenced in their electronic properties.

References

[1] P. R. Wallace. The Band Theory of Graphite. *Physical Review* **1947**, *71*, 622.

[2] R. Saito, M. Fujita, G. Dresselhaus, M. S. Dresselhaus. Electronic structure of chiral graphene tubules. *Applied Physics Letters* **1992**, *60*, 2204.

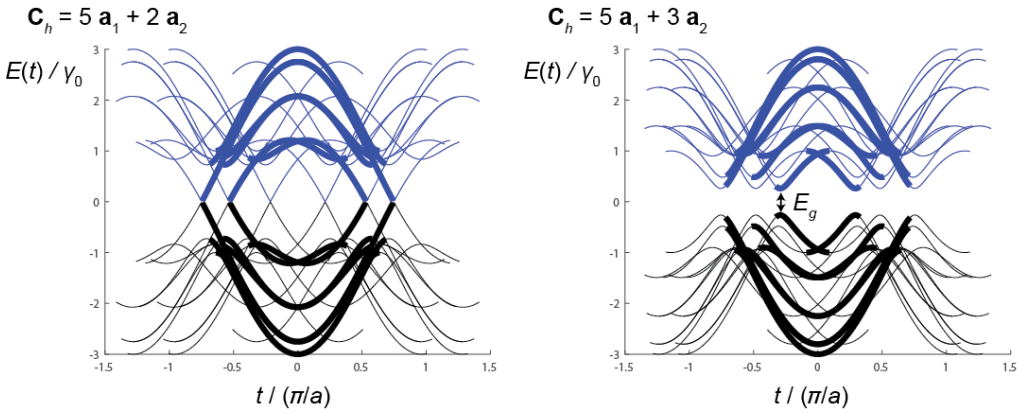

Figure 5: Dispersion E versus t for the (5,2) and (5,3) nanotubes discussed above. The different subbands are all plotted on the same axes, with portions of the subbands that fall within the Brillouin zone marked by thicker lines.

[3] A. H. Castro Neto, F. Guinea, N. M. R. Peres, K. S. Novoselov, A. K. Geim. The electronic properties of graphene. *Reviews of Modern Physics* **2009**, *81*, 109–162.